AMERICAN SOCIETY FOR MICROBIOLOGY | Journal of Bacteriology®

RESEARCH ARTICLE

A Putative Microcin Amplifies Shiga Toxin 2a Production of *Escherichia coli* O157:H7

Hillary M. Mosso,[a] Lingzi Xiaoli,[b]* Kakolie Banerjee,[b]* Maria Hoffmann,[c] Kuan Yao,[c] Edward G. Dudley[b,d]

[a]The Huck Institutes of the Life Sciences, The Pennsylvania State University, University Park, Pennsylvania, USA
[b]Food Science Department, The Pennsylvania State University, University Park, Pennsylvania, USA
[c]Center for Food Safety and Nutrition, U.S. Food and Drug Administration, College Park, Maryland, USA
[d]*E. coli* Reference Center, The Pennsylvania State University, University Park, Pennsylvania, USA

ABSTRACT *Escherichia coli* O157:H7 is a foodborne pathogen implicated in various multistate outbreaks. It encodes Shiga toxin on a prophage, and Shiga toxin production is linked to phage induction. An *E. coli* strain, designated 0.1229, that amplified Stx2a production when cocultured with *E. coli* O157:H7 strain PA2 was identified. Growth of PA2 in 0.1229 cell-free supernatants had a similar effect, even when supernatants were heated to 100°C for 10 min, but not after treatment with proteinase K. The secreted molecule was shown to use TolC for export and the TonB system for import. The genes sufficient for production of this molecule were localized to a 5.2-kb region of a 12.8-kb plasmid. This region was annotated, identifying hypothetical proteins, a predicted ABC transporter, and a cupin superfamily protein. These genes were identified and shown to be functional in two other *E. coli* strains, and bioinformatic analyses identified related gene clusters in similar and distinct bacterial species. These data collectively suggest that *E. coli* 0.1229 and other *E. coli* strains produce a microcin that induces the SOS response in target bacteria. Besides adding to the limited number of microcins known to be produced by *E. coli*, this study provides an additional mechanism by which stx_{2a} expression is increased in response to the gut microflora.

IMPORTANCE How the gut microflora influences the progression of bacterial infections is only beginning to be understood. Antibiotics are counterindicated for *E. coli* O157:H7 infections, limiting treatment options. An increased understanding of how the gut microflora directs O157:H7 virulence gene expression may lead to additional treatment options. This work identified *E. coli* strains that enhance the production of Shiga toxin by O157:H7 through the secretion of a proposed microcin. Microcins are natural antimicrobial peptides that target specific species, can act as alternatives to antibiotics, and mediate microbial competition. This work demonstrates another mechanism by which non-O157 *E. coli* strains may increase Shiga toxin production and adds to our understanding of microcins, a group of antimicrobials less well understood than colicins.

KEYWORDS *Escherichia coli*, O157:H7, Shiga toxins, bacteriocins, microcins

Escherichia coli O157:H7 is a notorious member of the enterohemorrhagic *E. coli* (EHEC) pathotype, which causes hemolytic colitis and hemolytic-uremic syndrome (HUS) through the production of virulence factors, including the locus of enterocyte effacement (LEE) and Shiga toxin (Stx) (1, 2). Stx is encoded on a lambdoid prophage (3). Induction of the prophage and subsequent upregulation of *stx* are tied to the activation of the bacterial SOS response (4). Therefore, DNA-damaging agents, including certain antibiotics, increase Stx synthesis and are typically counterindicated during treatment (5). There are two Stx types, referred to as Stx1 and Stx2 (6). Stx1 is further

Citation Mosso HM, Xiaoli L, Banerjee K, Hoffmann M, Yao K, Dudley EG. 2020. A putative microcin amplifies Shiga toxin 2a production of *Escherichia coli* O157:H7. J Bacteriol 202:e00353-19. https://doi.org/10.1128/JB.00353-19.

Editor Victor J. DiRita, Michigan State University

Address correspondence to Edward G. Dudley, egd100@psu.edu.

* Present address: Lingzi Xiaoli, Division of Bacterial Diseases, Centers for Disease Control and Prevention, Atlanta, Georgia, USA; Kakolie Banerjee, MilliporeSigma, Bedford, Massachusetts, USA.

Received 23 May 2019
Accepted 1 October 2019
Accepted manuscript posted online 14 October 2019
Published 6 December 2019

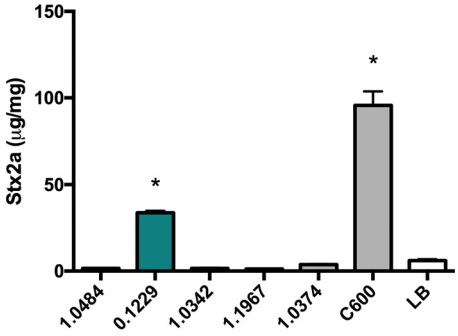

FIG 1 PA2 was grown with various *E. coli* strains, and Stx2a levels were measured using an R-ELISA. LB refers to PA2 grown in monoculture. One-way analysis of variance (ANOVA) was used, and bars marked with an asterisk show values that were significantly higher than for LB ($P < 0.05$ by Dunnett's test).

divided into three subtypes, Stx1a, Stx1c, and Stx1d (7). Stx2 also has multiple subtypes, designated Stx2a, Stx2b, Stx2c, Stx2d, Stx2e, Stx2f, Stx2g (7), Stx2h (8), and Stx2i (9). In general, infections caused by Stx1 and, interestingly, even those caused by both Stx1 and Stx2 (such as strains EDL933 [10] and Sakai [11]) are associated with less severe disease symptoms than Stx2-only-producing *E. coli* (12–14). Of the Stx2 subtypes, Stx2a is more commonly associated with clinical cases and instances of HUS (14–17). Indeed, the FAO and WHO consider STEC carrying stx_{2a} to be of the greatest concern (18).

Stx2a levels can be affected *in vitro* and *in vivo* when *E. coli* O157:H7 is cultured along with other bacteria. Indeed, it was found that stx_{2a} expression is downregulated by various probiotic species (19, 20) or in a medium conditioned with human microbiota (21). Conversely, nonpathogenic *E. coli* strains that are susceptible to infection by the stx_{2a}-converting phage were reported to increase Stx2a levels (22, 23). This mechanism is O157:H7 strain dependent (23) and requires the expression of *E. coli* BamA, which is the phage receptor (24, 25).

Production of Stx2a by O157:H7 is mediated by quorum sensing (26) and can also increase in response to molecules secreted by other members of the gut microbiota (24, 27), such as bacteriocins and microcins. Bacteriocins are proteinaceous toxins produced by bacteria that inhibit the growth of closely related bacteria. For example, a colicin E9 (ColE9)-producing strain amplified Stx2a when grown together with Sakai to higher levels than a colicin E3 (ColE3)-producing strain (27). ColE9 is a DNase, while ColE3 has RNase activity, and this may explain the differences in SOS induction and Stx2a levels. In support of this, the addition of extracted DNase colicins to various *E. coli* O157:H7 strains increased Stx2a, but not Stx1, production (27). Additionally, microcin B17 (MccB17), a DNA gyrase inhibitor, was shown to amplify Stx2a production (24). It was hypothesized that nonpathogenic *E. coli* strains could secrete additional colicins and microcins capable of increasing Stx2a production by O157:H7.

RESULTS

0.1229 amplifies Stx2a production in a cell-independent manner. Twelve human-associated *E. coli* isolates were tested for their ability to enhance Stx2a production in coculture with O157:H7. One of four amplifying isolates (data not shown), strain 0.1229, significantly increased Stx2a production of PA2, compared to PA2 alone (Fig. 1). C600 was included as a positive control, as it was previously shown to increase Stx2a production when cocultured with O157:H7 (22, 23).

Growth of PA2 in cell-free supernatants of 0.1229 also amplified Stx2a production, indicating that this phenomenon does not require whole cells (Fig. 2A). Sequencing of the genome of 0.1229 using Illumina technology revealed that it belonged to the same sequence type (ST73) as *E. coli* strains CFT073 (28) and Nissle 1917 (29) and carried a plasmid similar to pRS218 in *E. coli* RS218 (30). However, supernatants harvested after growth of these strains failed to increase Stx2a production by PA2 (Fig. 2A). To test whether increased Stx2a production was dependent on *recA*, 0.1229 was cocultured

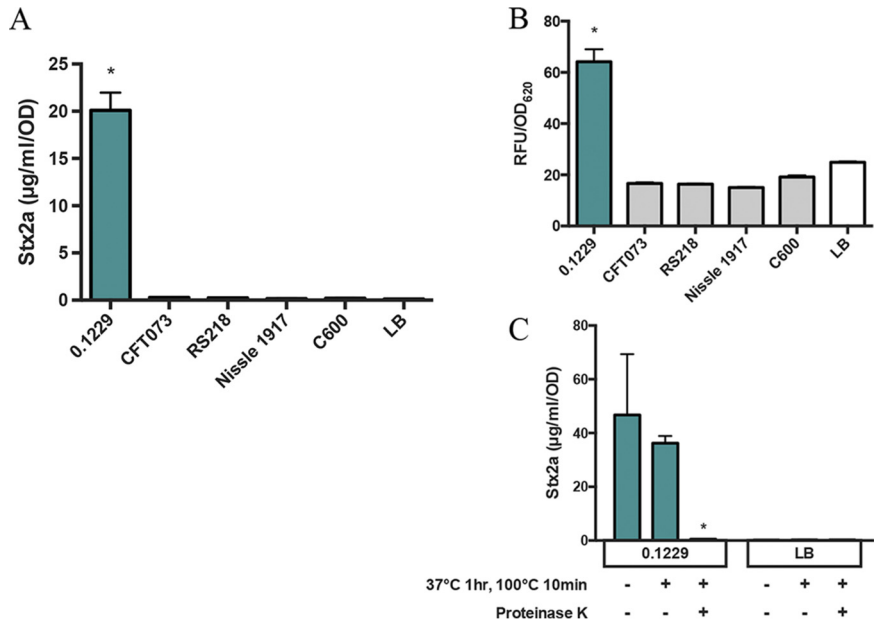

FIG 2 (A and B) Stx2a levels (A) and fluorescence (B) of nonpathogenic *E. coli*, after PA2 growth in the cell-free supernatant or W3110 Δ*tolC* P*recA-gfp* coculture, respectively. Samples were normalized to the OD_{600} or OD_{620} for Stx2a or fluorescence, respectively. One-way ANOVA was used, and levels marked with an asterisk were significantly higher than for LB ($P < 0.05$ by Dunnett's test). (C) Stx2a levels of PA2 grown in the 0.1229 cell-free supernatant (left) or LB (right), with or without heat and proteinase K treatments. Two-way ANOVA was used, and bars marked with an asterisk show values that were significantly lower than for untreated 0.1229 or LB ($P < 0.05$ by Dunnett's test).

with the W3110 Δ*tolC* P*recA-gfp* reporter strain. As anticipated, we found that among this collection, only strain 0.1229 increased green fluorescent protein (GFP) expression in coculture (Fig. 2B). Treatment of 0.1229 supernatants revealed that this bioactivity was resistant to boiling and sensitive to proteinase K (Fig. 2C). This phenotype is not unique to O157:H7 strain PA2, as EDL933 and C600 carrying the 933W stx_{2a}-converting phage also exhibit increased Stx2a production when grown in the supernatant of 0.1229 (see Fig. S1 in the supplemental material).

The plasmids of 0.1229 may play a role in Stx2a amplification. Further analysis of the Illumina sequence data revealed high sequence identity between the chromosome of 0.1229 and those of other *E. coli* isolates. CFT073 was 99.97% identical at the nucleotide level (97% query coverage), Nissle 1917 was 99.99% identical (96% query), and RS218 was 99.21% identical (93% query) to 0.1229, using BLAST. The most notable differences were in predicted plasmid content. To obtain a more complete picture, Pacific Biosciences (PacBio) long-read technology was used to sequence the genome of 0.1229.

The largest plasmid of 0.1229, designated p0.1229_1, was 114,229 bp and 99.99% identical with 100% query coverage to pUTI89 (31) and pRS218 (30) (Fig. S2A). A second plasmid, designated p0.1229_2, had five identifiable antimicrobial resistance genes, was 96,272 bp, and carried the operon for MccB17, a microcin that inhibits DNA gyrase (32). The plasmid p0.1229_2 shared high sequence identity with other known plasmids, being 99.96% identical with 57% query coverage to pRS218, 97.81% identical with 82% query coverage to pECO-fce (NCBI accession number CP015160), and 100% identical with 89% query coverage to pSF-173-1 (33) (Fig. S2B). A third plasmid was smaller than the cutoff for size selection used during PacBio library preparation; however, this sequence was identified within the Illumina sequence assemblies. This plasmid, designated p0.1229_3, was 12,894 bp and encoded ampicillin resistance (bla_{TEM-1b}) (Fig. S2C). It was similar to pEC16II (NCBI accession number KU932034), being 99.85% identical with 61% query coverage, and to pHUSEC41-3 (34), being 98.89% identical with 61% query coverage.

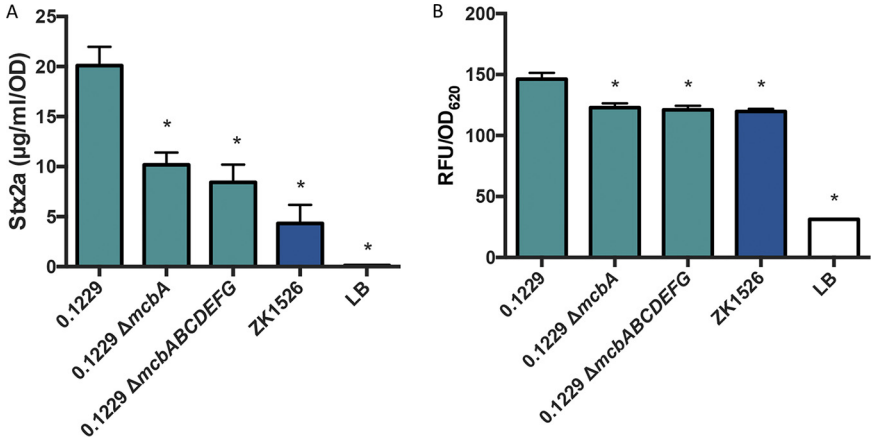

FIG 3 Stx2a levels (A) and fluorescence (B) of 0.1229, its MccB17 knockouts, and ZK1526, after PA2 growth in the cell-free supernatant or W3110 Δ*tolC* P*recA-gfp* coculture, respectively. Samples were normalized to the OD_{600} or OD_{620} for Stx2a or fluorescence, respectively. One-way ANOVA was used, and bars marked with an asterisk show values that were significantly lower than for 0.1229 ($P < 0.05$ by Dunnett's test).

As RS218 did not amplify Stx2a production (Fig. 2A), it was assumed that p0.1229_1 did not carry the genes responsible for this phenotype. Similarly, *E. coli* strain SF-173 did not increase GFP levels when cocultured with W3110 Δ*tolC* P*recA-gfp*, suggesting that genes carried on p0.1229_2 were also not required (data not shown).

Strain 0.1229 encodes microcin B17, which is partially responsible for Stx2a amplification. MccB17 is a 3.1-kDa (43-amino-acid) DNA gyrase inhibitor; its gene is found on a seven-gene operon, with *mcbA* encoding the 69-amino-acid microcin precursor (32). Although pSF-173-1 carries this operon, there was a 3-nucleotide deletion observed in *mcbA* in pSF-173-1, compared to a previously reported sequence (32). This deletion is predicted to shorten a 10-Gly homopolymeric stretch by 1 amino acid residue. Although this Gly-rich region is not important for interaction with the gyrase-DNA complex (35), it seemed prudent to confirm that the results reported above for strain SF-173 were not due to the production of a nonfunctional McbA. Therefore, knockouts of *mcbA* (Δ*mcbA*) and the entire operon (Δ*mcbABCDEFG*) were constructed in 0.1229. These mutations decreased Stx2a amplification by O157:H7 compared to wild-type 0.1229 (Fig. 3A); however, they did not ablate the Stx2a levels back to monoculture levels. Similar results were seen with the P*recA-gfp* strain (Fig. 3B), although differences were less pronounced than those seen with the Stx assays.

Four ORFs carried by p0.1229_3 are necessary for the Stx2a amplification phenotype. To identify the other factors encoded on p0.1229_3 that affect Stx2a amplification, p0.1229_3 was transformed into strain C600. Spent supernatants from C600(p0.1229_3) were found to amplify Stx2a production of PA2 (Fig. 4), confirming the importance of this plasmid. By systematically deleting portions of p0.1229_3, two regions were identified as being essential for increased Stx2a production (Fig. 5A). The genes annotated in these regions are referred to as those for hypothetic proteins (Hps), domains of unknown function (DUF), an ATP-binding cassette (ABC)-type transporter, and a member of the cupin superfamily of conserved barrel domains. The mutant, 0.1229Δ6 (bp 2850 to 5473), deleted two open reading frames (ORFs), referred to as Hp1 and ABC ORFs, and 0.1229Δ7 (bp 5426 to 7950) deleted cupin, DUF4440, DUF2164, Hp2, Hp3, and a portion of a predicted nuclease (Fig. 5B). These results were confirmed using coculture assays with the P*recA-gfp* reporter (Fig. S3A). Insertional inactivation of individual ORFs in these regions identified four, Hp1, ABC, cupin, and Hp2 ORFs, that were necessary for enhanced Stx2a production (Fig. 5C). Similar results were shown for cocultures with P*recA-gfp*, although 0.1229 Hp2 showed only a moderate decrease in GFP expression (Fig. S3B). Cloning of a 5.2-kb region of the plasmid, spanning upstream of HP1 through the beginning of the putative nuclease-encoding gene, confirmed that

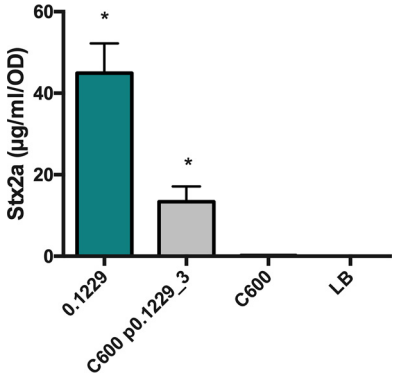

FIG 4 PA2 was grown in the cell-free supernatants of 0.1229, C600 containing p0.1229_3, and C600. Stx2a levels were measured using an R-ELISA. LB refers to PA2 grown in LB. One-way ANOVA was used, and bars marked with an asterisk show values that were significantly higher than for LB ($P < 0.05$ by Fisher's least significant difference [LSD] test).

this activity is encoded within this region (Fig. 5D). Cloning of a similar region that ended after *abc* did not provide C600 the ability to increase GFP levels (data not shown).

In silico comparisons identified a nearly identical gene cluster in other species, including *Shigella sonnei* and *Klebsiella pneumoniae* (Fig. S4). The region of p0.1229_3 spanning bp 2745 to 7238 was >99.6% identical at the nucleotide level, comparing all the strains in Fig. S2. Similar gene clusters containing Hp1 at 36 to 68% amino acid identity were found in other species as well (Fig. S5). In these clusters, orthologs of Hp1,

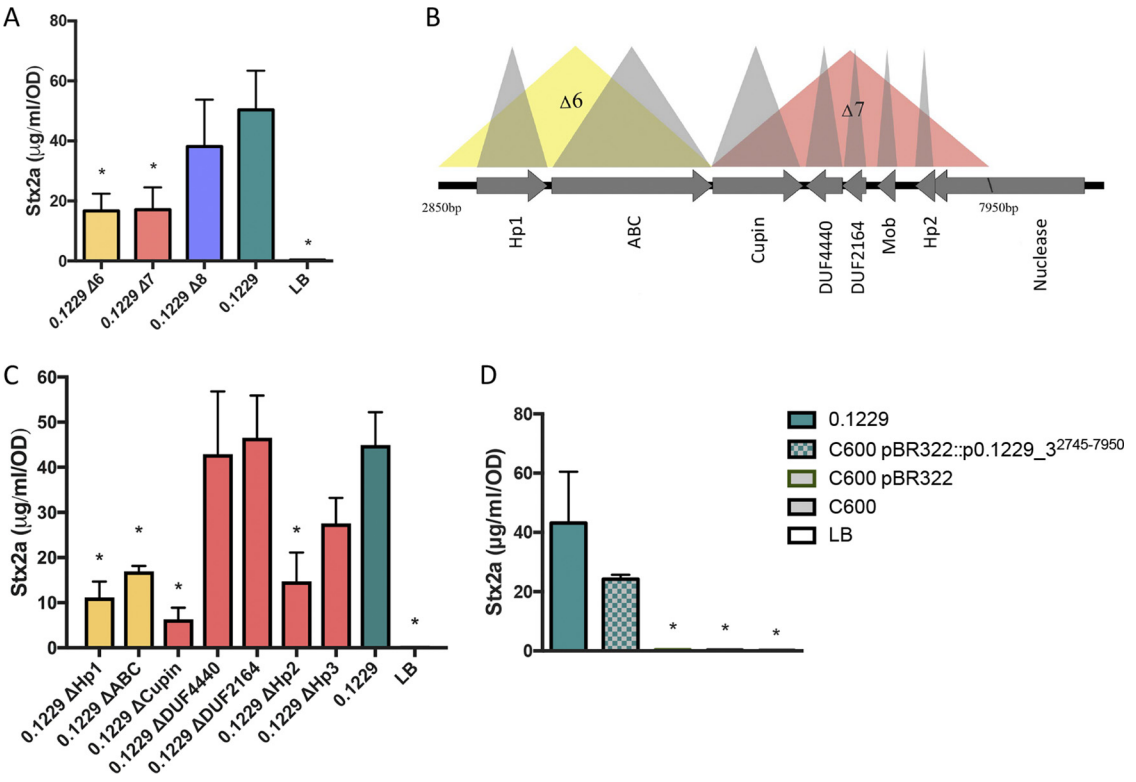

FIG 5 (A and C) PA2 was grown in the cell-free supernatants of 0.1229 knockouts. (B) Depiction of a portion of p0.1229_3 with predicted open reading frames (ORFs). The colored triangles indicate the name of the regional knockout. (D) PA2 grown in the supernatant of a C600 strain containing a portion of p0.1229_3 (pBR322::p0.1229_3$^{2745–7950}$). Stx2a levels were measured using an R-ELISA. LB refers to PA2 grown in LB. One-way ANOVA was used, and bars marked with an asterisk show values that were significantly lower than for 0.1229 ($P < 0.05$ by Fisher's LSD test).

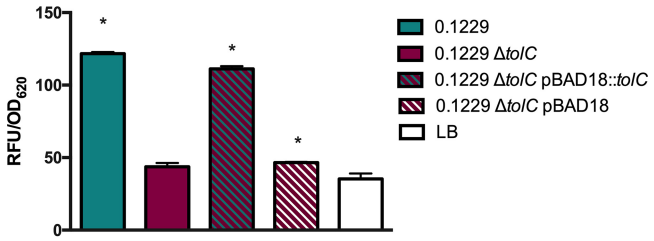

FIG 6 W3110 Δ*tolC* P*recA-gfp* was grown in coculture with the 0.1229, 0.1229 Δ*tolC*, and 0.1229 Δ*tolC* pBAD18-containing strains, and fluorescence was measured. Samples were normalized to the OD_{620}. One-way ANOVA was used, and bars marked with an asterisk show values that were significantly higher than for LB ($P < 0.05$ by Dunnett's test).

ABC, and cupin genes were commonly colocalized, and the genes were found in the same order.

The secreted molecule requires *tolC* for secretion and *tonB* for import into target strains. Some bacteriocins and microcins require genes located outside the main operon for secretion, such as the efflux protein TolC (36). The supernatant of 0.1229 Δ*tolC* did not increase Stx2a expression by strain PA2 to levels seen with wild-type 0.1229 supernatants (data not shown). Similar results were observed in coculture experiments using the P*recA-gfp*-carrying strain (Fig. 6). The phenotype was restored when *tolC* was complemented on a plasmid but only when tested with the P*recA-gfp* strain (Fig. 6). Similarly, numerous bacteriocins are translocated into target cells using the TonB system (37). A *tonB* knockout was constructed in the P*recA-gfp* reporter strain, as we were unsuccessful in generating this in a O157:H7 background. In coculture with 0.1229, the MG1655 Δ*tonB* P*recA-gfp* strain produced lower GFP levels than the MG1655 P*recA-gfp* strain (Fig. 7). This phenotype was restored when pBAD24::*tonB*, but not pBAD24, was transformed into the mutant strain (Fig. 7).

Identification of the gene cluster in additional strains. Finally, it was hypothesized that *E. coli* strains isolated from human feces would encode molecules similar to the ones identified here. A total of 101 human fecal *E. coli* isolates were obtained from Penn State's *E. coli* Reference Center, and three of these were found to induce GFP production in the P*recA-gfp* reporter assay (Fig. S6). Furthermore, the supernatants of two of these isolates, designated 91.0593 and 99.0750, increased Stx2a to levels similar to those in 0.1229; however, 90.2723 did not (Fig. 8A). Genome sequencing of these three organisms revealed that 91.0593 and 99.0750 carried plasmids similar to p0.1229_3; however, the latter plasmid had a deletion in the recombinase and transposon regions (Fig. 8B). Strain 99.0750 was of molecular serotype O36:H39, while 91.0593 could not be O typed but was identified as H10. Reads from 824 *E. coli* isolates (Table S1) were screened for the nucleotide sequence of the putative gene cluster, including Hp1, ABC, and cupin genes. However, none of the *E. coli* isolates tested carried this region.

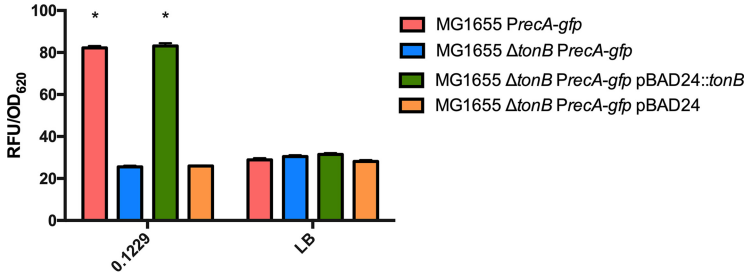

FIG 7 A plasmid expressing P*recA-gfp* was electroporated into MG1655, MG1655 Δ*tonB*, MG1655 Δ*tonB*(pBAD24), and MG1655 Δ*tonB*(pBAD24::*tonB*). These strains were grown in coculture with 0.1229 or by themselves (LB). Two-way ANOVA was used, and bars marked with an asterisk show values that were significantly higher than for their respective monoculture controls ($P < 0.05$ by Dunnett's test).

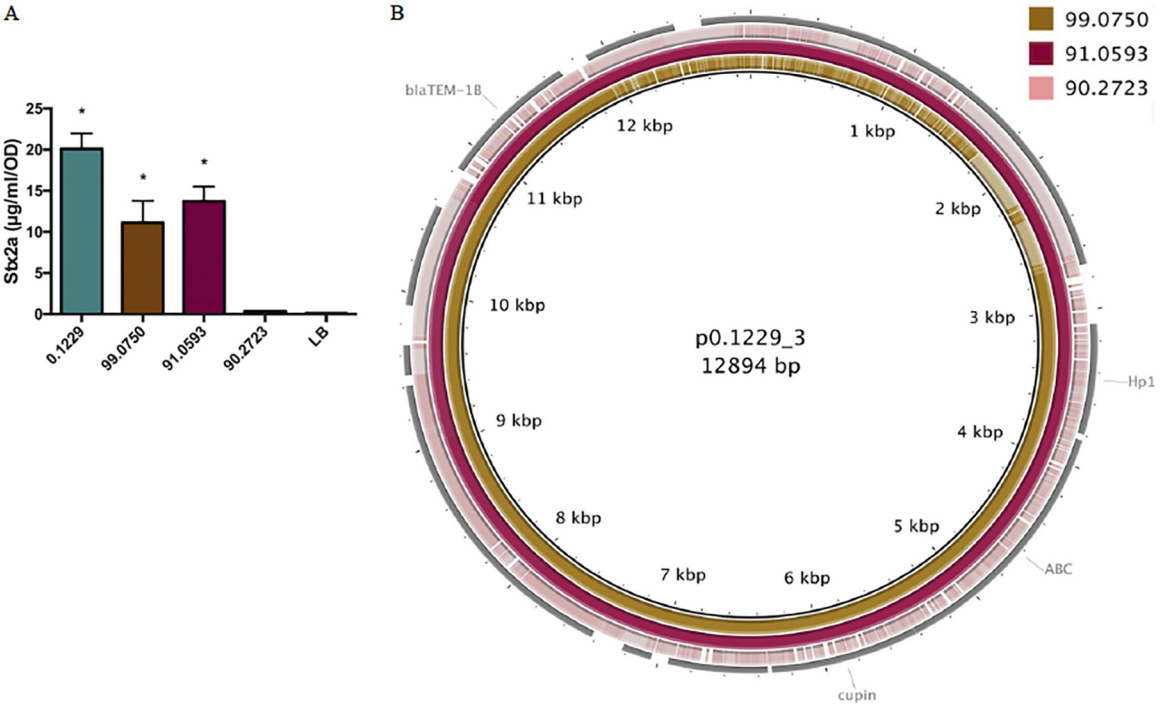

FIG 8 (A) PA2 was grown in the cell-free supernatants of 0.1229 and three human fecal *E. coli* isolates. Stx2a levels measured using an R-ELISA. LB refers to PA2 grown in LB. One-way ANOVA was used, and bars marked with an asterisk show values that were significantly higher than for LB ($P < 0.05$ by Dunnett's test). (B) p0.1229_3 was compared to the contigs of 99.0750, 91.0593, and 90.2723 using BLAST and visualized using BRIG.

DISCUSSION

The concentration of *E. coli* in human feces ranges from 10^7 to 10^9 CFU (38, 39). Typically, there are up to five commensal *E. coli* strains colonizing the human gut at a given time (40, 41). As the human microbiota affects O157:H7 colonization and virulence gene expression (42–45), it is thought that community differences in the gut microflora may explain, in part, individual differences in disease symptoms (46). Indeed, commensal *E. coli* strains can be susceptible to stx_2-converting phage and increase phage and Stx production (22, 23). In mice given a coculture of O157:H7 and phage-resistant *E. coli*, minimal toxin was recovered in the feces, but with *E. coli* strains that were phage susceptible, higher levels of toxin were found (47). However, it is clear that phage infection of susceptible bacteria is not the only mechanism by which the gut microflora affects Stx2 levels during infection (19, 20, 24, 27).

In this study, both whole cells and spent supernatants of *E. coli* 0.1229 enhanced Stx2a production by *E. coli* O157:H7 strain PA2. The latter strain is a member of the hypervirulent clade 8 (48) and was previously found to be a high-Stx2a producer in coculture with *E. coli* C600 (23) by a mechanism distinct from the one described here. *E. coli* 0.1229 produces at least two molecules capable of increasing Stx2a levels. The first is MccB17, a DNA gyrase inhibitor shown to activate Stx2a production in a previous study (24). The present study identified a second molecule localized to a 12.8-kb plasmid, and all genes necessary for production are found within a 5.2-kb region. Furthermore, gene knockouts identified four potential ORFs within this region, Hp1, ABC, cupin, and Hp2 ORFs, that are required for 0.1229-mediated Stx2a amplification. This gene cluster was also identified on pB51 (49), a plasmid similar to p0.1229_3; however, limited characterization was reported.

Oxidizing agents, such as hydrogen peroxide (H_2O_2), and antibiotics targeting DNA replication, such as ciprofloxacin, mitomycin C, and norfloxacin, are known to induce *stx*-converting phage (5, 50, 51) and, subsequently, Stx2 production (5, 50). However, the Stx2-amplifying activity of the 0.1229 supernatant was abolished by proteinase K,

suggesting that the inducing molecule is proteinaceous in nature. *Coli*cins are bacteriocins found in *E. coli* (52) and are generally >30 kDa, and at least one member has been previously shown to enhance O157:H7 Stx2 production (27). While some colicins utilize TonB for translocation, they are not expected to be heat stable. The molecule produced by 0.1229 was resistant to 100°C for 10 min, strongly suggesting that it is not a colicin.

Microcins are bacteriocins that are generally smaller than 10 kDa (94). Their size and lack of secondary and tertiary structures make them more heat stable than colicins. Microcins are divided into three classes; members of class I and class IIa are plasmid encoded, while members of class IIb are chromosomally encoded. Members of class I and IIb are posttranslationally modified (53, 54), while members of class IIa are not. To date, all members of class II, but only one member of class I (microcin J25 [MccJ25]), use an ABC-type transporter in complex with TolC for export (36) and the TonB system for import into target cells (37). The putative microcin produced by 0.1229 is plasmid encoded, along with a predicted ABC transporter, and is TolC and TonB dependent. Therefore, this microcin appears to be more closely related to class IIa microcins. However, purification of the microcin to identify possible posttranslational modifications is necessary to confirm whether designating it as belonging to class I or IIa is more appropriate.

There are four known class IIa microcins, microcin V (MccV) (previously named colicin V) (55, 56), microcin N (MccN) (previously named Mcc24) (57), microcin L (MccL) (58), and microcin PDI (MccPDI) (59, 60). The operons encoding these microcins contain four or five genes, including the microcin precursor, immunity, and export genes. The MccN operon also encodes a putative regulator with a histone-like nucleoid domain (57). The microcin precursors possess leader sequences of approximately 15 amino acids, containing the signature sequence MRXI/LX_9GG/A (where X is any amino acid), and are typically cleaved by the ABC transporters during export (61). A potential leader sequence with a double glycine was found in Hp2. Additionally, a small peptide (DHGSR) was identified in the supernatants of 0.1229 by mass spectroscopy (data not shown), corresponding to an ORF internal to the Hp2 ORF, encoded in the opposite direction. Future experiments will determine if one of these, or another region, encodes a secreted microcin.

One argument against designation as a class IIa microcin is the lack of an identifiable N-terminal proteolytic domain (62) in the predicted ABC transporter encoded on p0.1229_3. This domain is found in all other members of class IIa. Interestingly, the class I MccJ25 operon also encodes an ABC transporter lacking this domain. Unlike the other class I microcins, MccJ25 is TolC and TonB dependent for export and import, respectively. While the possibility that the system identified here is a class I microcin cannot be excluded, if so, it is more similar to MccJ25 than to other members of this group.

While the current mechanism of action is unknown, it is theorized that the putative microcin causes DNA damage through double-strand breaks, depurination, or inhibition of DNA replication. Such actions would lead to RecA-dependent phage induction and Stx2 production. The suspected mode of action would be divergent from those of the known class IIa microcins, which target the inner membrane (63), and MccJ25, which inhibits the RNA polymerase (64). Besides the predicted ABC transporter, the functions of the other ORFs are unclear. We anticipate that one of these may encode an ABC accessory protein known to be essential for these export complexes (65). One ORF encodes a cupin domain found in a functionally diverse set of proteins. An immunity gene protecting the host may also be expected in this region.

The genes encoding the putative microcin were additionally found in *E. coli* strains 99.0750 and 91.0593. Genome sequencing of these strains failed to identify genes encoding MccB17, which may explain the lower levels of Stx2a production seen in coculture with PA2 than those seen with 0.1229. Bioinformatic analyses also identified other *E. coli* strains that encode nearly identical regions. Interestingly, one of these was *E. coli* O104:H4 HUS, isolated in 2001 (34) and responsible for a large 2011 outbreak in Germany. However, a premature stop codon identified in the cupin gene suggests that

it is nonfunctional. Homologs of the Hp1, ABC, and cupin genes were identified together in several other organisms distantly related to *E. coli*, suggesting that they encode a functional unit. The absence of the Hp2 ORF in most of these genetic clusters argues against this ORF encoding the antibacterial activity or may suggest that these organisms encode microcins distinct from Hp2. This putative microcin is more prevalent in human *E. coli* isolates than in environmental, animal, and food isolates, possibly explaining why it was only recently discovered.

In conclusion, a putative microcin was identified in *E. coli*, expanding our knowledge of this small group of antimicrobial peptides. This study also identifies another mechanism by which *E. coli* may enhance Stx2a production by *E. coli* O157:H7. Further studies may also provide new insights into the diverse genetic structures and functions of microcin-encoding systems.

MATERIALS AND METHODS

Bacterial strains, media, and growth conditions. *E. coli* strains were grown in lysogeny broth (LB) at 37°C unless otherwise indicated, and culture stocks were maintained in 20% glycerol at −80°C. The following antibiotics were used at the indicated concentrations: ampicillin (100 μg/ml), chloramphenicol (25 μg/ml), kanamycin (50 μg/ml), and tetracycline (10 μg/ml). All bacterial isolates, plasmids, and primers used in this study can be found in Tables 1 and 2. *E. coli* SF-173-1 was provided by Craig Stephens, Santa Clara University.

Coculture with PA2. Coculture with *E. coli* O157:H7 PA2 was performed using methods similar to ones described previously (23). PA2 and commensal *E. coli* strains were grown overnight at 37°C (with shaking at 250 rpm). LB (2.5 ml) was added to 6-well plates (BD Biosciences Inc., Franklin Lakes, NJ) and allowed to solidify. PA2 and commensal strains were each diluted to an optical density at 600 nm (OD_{600}) of 0.05 in 1 ml of LB and added to the 6-well plates. A monoculture of PA2 (at an OD_{600} of 0.05 in 1 ml) served as a negative control. The plates were incubated without shaking at 37°C. After 16 h, cultures were collected, cells were lysed with 6 mg/ml polymyxin B at 37°C for 5 min, and supernatants were collected. Samples were immediately tested with a receptor-based enzyme-linked immunosorbent assay (R-ELISA), as described below, or stored at −80°C. The total protein concentration was calculated using the Bradford assay (VMR Life Science, Philadelphia, PA) and used to calculate the concentration of Stx2 in micrograms per milligram.

R-ELISA for Stx2a detection. Detection of Shiga toxin was performed using a sandwich ELISA approach previously described by Xiaoli et al. (24). Briefly, 25 μg/ml of ceramide trihexosides (bottom spot) (Matreya Biosciences, Pleasant Gap, PA) dissolved in methanol was used for coating of the plate. Washes were performed between each step by using phosphate-buffered saline (PBS) and 0.05% Tween 20. Stx2a-containing samples were diluted in PBS as necessary to obtain final readings in the linear range. Samples were added to the wells in duplicate and incubated with shaking for 1 h at room temperature. Supernatants of *E. coli* PA11, a high-Stx2a producer (66), were used as a positive control. Anti-Stx2 monoclonal mouse antibody (Santa Cruz Biotech, Santa Cruz, CA) was added to the plate at a concentration of 1 μg/ml, and the plate was then incubated for 1 h. Anti-mouse secondary antibody (MilliporeSigma, Burlington, MA) conjugated to horseradish peroxidase (1 μg/ml) was added to the plate, and the plate was incubated for 1 h. For detection, one-step Ultra-TMB (Thermo Fisher, Waltham, MA) was used, and 2 M H_2SO_4 was added to the wells to stop the reaction. The plate was read at 450 nm using a DU 730 spectrophotometer (Beckman Coulter, Atlanta, GA). A standard curve was generated from 2-fold serially diluted PA11 samples and used to quantify the concentration (in micrograms per milliliter) of Stx2a present in each sample.

Cell-free supernatant assay with PA2. *E. coli* O157:H7 strain PA2 and nonpathogenic *E. coli* strains were individually grown with shaking at 37°C for 16 h. Cultures of the nonpathogenic strains grown overnight were centrifuged, and supernatants were filtered through 0.2-μm cellulose filters (VWR International, Radnor, PA). LB agar (2.5 ml) was added to the wells of 6-well plates (BD Biosciences Inc., Franklin Lakes, NJ) and allowed to solidify. PA2 was added to wells at a final OD_{600} of 0.05 in 1 ml of the spent supernatant. For the negative control, PA2 was resuspended in fresh LB to the same cell density, and 1 ml was added to a well. The plates were statically incubated at 37°C for 8 h, after which the cell density (OD_{600}) was recorded. Cells were lysed with 6 mg/ml polymyxin B at 37°C for 5 min, and the supernatant was recovered. Samples were immediately tested for Stx2a by an R-ELISA or stored at −80°C. Data are reported as micrograms per milliliter per OD_{600} unit.

Detection of SOS-inducing agents using P*recA-gfp*. *E. coli* expressing P*recA-gfp*, which encodes green fluorescent protein (GFP) under the control of the *recA* promoter (67), was purchased from Dharmacon (Lafayette, CO). The plasmid was transformed into *E. coli* W3110 Δ*tolC*. The *tolC* deletion reduces the potential efflux of *recA*-activating molecules. W3110 Δ*tolC* P*recA-gfp* and commensal strains were individually grown overnight with shaking at 37°C. LB agar (2.5 ml) was added to 6-well plates and allowed to solidify. W3110 Δ*tolC* P*recA-gfp* and one commensal strain were each diluted to a final OD_{600} of 0.05 in LB, and 1 ml was added to the 6-well plates. The negative control included only W3110 Δ*tolC* P*recA-gfp* at a final OD of 0.05 in 1 ml LB. The plates were statically incubated at 37°C. After 16 h, 100 μl was removed from each well and added to black 96-well clear-bottom plates (Dot Scientific Inc., Burton, MI), and the OD_{620} was read using a DU 730 spectrophotometer. Relative fluorescence units (RFU) were measured at an excitation wavelength of 485 nm and an emission wavelength of 538 nm on a Fluoroskan

TABLE 1 Bacterial isolates and plasmids used in this study[a]

Strain or plasmid	Characteristic(s)	Reference or source
E. coli strains		
PA2	stx_{2a}; O157:H7; Pennsylvania	66
PA8	stx_{2a}; O157:H7; Pennsylvania	66
EDL933	stx_{2a} stx_{1a}; O157:H7	86
C600	K-12 derivative	87
MG1655	K-12 derivative	88
1.0484	A phylogroup; O147; Minnesota	ECRC
0.1229	B2 phylogroup; O18:H1; Amp^r Tet^r; ST73; California	ECRC
1.0342	D phylogroup; O11; Minnesota	ECRC
1.1967	B2 phylogroup; O21; Minnesota	ECRC
1.0374	D phylogroup; O77; Minnesota	ECRC
Nissle 1917	Mutaflor; O6:H1; ST73	29
CFT073	UPEC; O6:H1; ST73	28
RS218	NMEC; O18:H7; ST95	89
99.0750	O36:H39; Brazil	ECRC
91.0593	O?:H10; Mexico	ECRC
90.2723	O?:H12; New York	ECRC
ZK1526	Microcin B17-producing strain; W3110 Δ*lacU169 tna-2* pPY113; Amp^r	90
Derivatives		
0.1229 Δ*mcbA*	0.1229 Δ*mcbA*::*cat*; Cat^r Amp^r Tet^r	This study
0.122 Δ*mcbABCDEFG*	0.1229 Δ*mcbABCDEFG*::*cat*; Cat^r Amp^r Tet^r	This study
0.1229Δ6	0.1229 Δp0.1229_3$^{2850–5473}$::*cat*; Cat^r Amp^r Tet^r	This study
0.1229Δ7	0.1229 Δp0.1229_3$^{5426–7950}$::*cat*; Cat^r Amp^r Tet^r	This study
0.1229Δ8	0.1229 Δp0.1229_3$^{8001–9950}$::*cat*; Cat^r Amp^r Tet^r	This study
0.1229 Δ*hp1*	0.1229 Δp0.1229_3$^{3084–3792}$::*cat*; Cat^r Amp^r Tet^r	This study
0.1229 Δ*abc*	0.1229 Δp0.1229_3$^{3831–5423}$::*cat*; Cat^r Amp^r Tet^r	This study
0.1229 Δ*cupin*	0.1229 Δp0.1229_3$^{5426–6319}$::*cat*; Cat^r Amp^r Tet^r	This study
0.1229 Δ*DUF4440*	0.1229 Δp0.1229_3$^{6706–6344}$::*cat*; Cat^r Amp^r Tet^r	This study
0.1229 Δ*DUF2164*	0.1229 Δp0.1229_3$^{6942–6703}$::*cat*; Cat^r Amp^r Tet^r	This study
0.1229 Δ*hp2*	0.1229 Δp0.1229_3$^{7227–7048}$::*cat*; Cat^r Amp^r Tet^r	This study
0.1229 Δ*hp3*	0.1229 Δp0.1229_3$^{9099–7546}$::*cat*; Cat^r Amp^r Tet^r	This study
0.1229 Δ*tolC*	0.1229 Δ*tolC*::*cat*; Cat^r Amp^r Tet^r	This study
0.1229 Δ*tolC*(pBAD18::*tolC*)	0.1229 Δ*tolC*::*cat* + pBAD18::*tolC*; Cat^r Amp^r Tet^r Kan^r	This study
0.1229 Δ*tolC*(pBAD18)	0.1229 Δ*tolC*::*cat* + pBAD18; Cat^r Amp^r Tet^r Kan^r	This study
W3110 Δ*tolC* P*recA-gfp*	W3110 Δ*tolC*::*tet* + P*recA-gfp*; Tet^r Kan^r	67
MG1655 P*recA-gfp*	MG1655 P*recA-gfp*; Kan^r	This study
MG1655 Δ*tonB* P*recA-gfp*	MG1655 Δ*tonB*::*cat* + P*recA-gfp*; Cat^r Kan^r	This study
MG1655 Δ*tonB* P*recA-gfp*(pKP315)	MG1655 Δ*tonB*::*cat* + P*recA-gfp* + pKP215; Cat^r Kan^r Amp^r	This study
MG1655 Δ*tonB* P*recA-gfp*(pBAD24)	MG1655 Δ*tonB*::*cat* + P*recA-gfp* + pBAD24; Cat^r Kan^r Amp^r	This study
C600(pBR322::p0.1229_3$^{2745–7950}$)	C600 + pBR322::p0.1229_3$^{2745–7950}$; Tet^r	This study
C600(pBR322)	C600 + pBR322; Amp^r Tet^r	This study
C600(p0.1229_3)	C600 + p0.1229_3; Amp^r	This study
Plasmids		
p0.1229_1	114-kb plasmid of 0.1229	This study
p0.1229_2	96-kb plasmid of 0.1229; Tet^r	This study
p0.1229_3	13-kb plasmid of 0.1229; Amp^r	This study
pKD3	pKD3; Cat^r Amp^r	69
pKD46-Kan^R	pKD46; P_{araC}-λ red recombinase; Kan^r	Laboratory stocks
P*recA-gfp*	pMSs201 + P*recA-gfp*; Kan^r	67
pBAD24	pBAD24; *araC*; Amp^r	91
pKP315	pBAD24::*tonB*; P_{araC}; Amp^r	92
pBAD18	pBAD18; P_{araC}; Kan^r	91
pBAD18::*tolC*	pBAD18::*tolC*; P_{araC}; Kan^r	This study
pBR322	pBR322; Amp^r Tet^r	93
pBR322::hp1end7	pBR322::p0.1229_3$^{2850–7950}$; Tet^r	This study

[a]ECRC, Penn State *E. coli* Reference Center; Amp^r, ampicillin resistant; Cat^r, chloramphenicol resistant; Kan^r, kanamycin resistant; Tet^r, tetracycline resistant; stx_{2a}, Shiga toxin 2a gene; stx_{1a}, Shiga toxin 1a gene; P_{araC}, arabinose-inducible promoter; UPEC, uropathogenic *E. coli*; NEMC, neonatal meningitis *Escherichia coli*. Superscript numbers indicate regions that are knocked out.

Ascent FL instrument (Thermo Fisher Scientific, Waltham, MA) (68). RFU values were normalized to the cell density.

One-step recombination for *E. coli* knockouts. Mutants of 0.1229 and MG1655 were constructed using one-step recombination (69). Primers contained either 50 bp upstream or downstream of the gene of interest, followed by sequences annealing to the P1 and P2 priming sites from pKD3. PCR was performed with the following settings: an initial denaturation step at 95°C for 30 s; 10 cycles of 95°C for

TABLE 2 Primers used in this study[a]

Target(s)	Primer	Sequence	T_a, variable time
Δ*mcbA* and Δ*mcbABCDEFG*	mcbA-KF	atactattcagatgtcataagcattaatttcccttaaaaaaggagtccttGTGTAGGCTGGAGCTGCTTC	62°C, 100 s
	mcbA-KR	ttttttaatatcagggagcaccatgctccctgaacggttaattcaacgtaCATATGAATATCCTCCTTAG	
Δ*mcbA*	mcbA-VF	GGGGCTTAAAGGGGTAGTGT	49°C, 45 s
	mcbA-VR	AAGCGATTCGTCCAGTAGTTT	
Δ*mcbABCDEFG*	mcbG-KR	gtccggttctgaggaggggcccgtccgggcaaccggcgggtctactcaccCATATGAATATCCTCCTTAG	70.9°C, 2 min
	mcbG-VR	CCTAACAACGCCACGACTTT	49°C, 2 min
Δ6	6-KF	acacatttcgtacagcctttacactcggtgaattagcggccctagatgcaGTGTAGGCTGGAGCTGCTTC	67°C, 3 min
	6-KR	ttaaacctcatgttttgtgatatctataatctgtgctttaggtatattatCATATGAATATCCTCCTTAG	
	6-VF	GAAGATATCGCACGCCTCTC	54.5°C, 3 min
	6-VR	CGCCTGTTTGGCTATATGTG	
Δ7	7-KF	aatatacctaaagcacagattatagatatcacaaaacatgaggtttaaaaGTGTAGGCTGGAGCTGCTTC	70°C, 90 s
	7-KR	tggagtttgtgcaggacgggagaaggaaatttctggttatcccgcaggggCATATGAATATCCTCCTTAG	
	7-VF	TTCGATGAACCGACAAAAGG	54°C, 2.5 min
	7-VR	GGGTGAAAGAGGCGATGAT	
Δ8	8-KF	tttaccgcagctgcctcgcacgcttcggggatgacggtgaaaacctctgaGTGTAGGCTGGAGCTGCTTC	68°C, 90 s
	8-KR	agcagacaccgctcgccgcagccgaacgaccgagtgtagctagtcagtgaCATATGAATATCCTCCTTAG	
	8-VF	CACGGAGGCATCAGTGACTA	54.9°C, 2.5 min
	8-VR	CAGCCTTTTCCTGGTTCTTG	
ΔABC	ABC-KF	aattctagataacataaagcccgtaatatacgggctttaaggattataaaGTGTAGGCTGGAGCTGCTTC	64.5°C, 90 s
	ABC-KR	atatttcttaaatttttctatgatttccttttttataagattattcatttCATATGAATATCCTCCTTAG	
	ABC-VF	GCGAAAAGATGTTTGGAATGA	52.7°C, 90 s
	ABC-VR	TCGGGAAAGTTGTCATTTGC	
ΔHp1	hp1-KF	ataaatgataactattctcatctacattcaaatatataattgggggtgttGTGTAGGCTGGAGCTGCTTC	65.7°C, 90 s
	hp1-KR	aataaaattcaatttataatccttaaagcccgtatattacgggctttatgCATATGAATATCCTCCTTAG	
	hp1-VF	ACTGGCTGCAAAAACCTTGT	53.2°C, 75 s
	hp1-VR	TTTCTCCTATTGAATCTTTATTGTCA	
ΔCupin	cupin KF	aatatacctaaagcacagattatagatatcacaaaacatgaggtttaaaaGTGTAGGCTGGAGCTGCTTC	66.5°C, 3 min
	cupin KR	agtttatatcgtatgaaaaaatctaaggggaagccccttagattaatggCATATGAATATCCTCCTTAG	
	cupin VF	AAAGAGGAAAACAAGGAAAAGCA	54°C, 2 min
	cupin VR	GCATTGCTTGTGTTTCAGGG	
ΔDUF4440	DUF4440 KF	aaaaaataaaacttgaacatatataaccattaatctaaggggcttccccGTGTAGGCTGGAGCTGCTTC	68°C, 3 min
	DUF4440 KR	aggaatgttggggatagattagaggaggaattagatatgaggaaggtagtCATATGAATATCCTCCTTAG	
ΔDUF2164	DUF2164 KF	tgcattataccattcttttcttattagatttaagtctgatttaaaattagGTGTAGGCTGGAGCTGCTTC	68°C, 3 min
	DUF2164 KR	tgataggaaaaatgttatattattaatttatttgtgaggcttcataaagaCATATGAATATCCTCCTTAG	
ΔDUF4440 and ΔDUF2164	DUF4440/2164 VF	GGCACAATGTTACGACTCAGA	55°C, 90 s
	DUF4440/2164 VR	GTTTCAGCGGTGCGTACAAT	
ΔHp2	hp2 KF	aaattacaactcaaccatactgcaacctggaatttcccaagcaagcatatGTGTAGGCTGGAGCTGCTTC	68°C, 3 min
	hp2 KR	tgtctctggctggcaattcctgcgtgattcacatggctgcatagctatgcCATATGAATATCCTCCTTAG	
	hp2 VF	TCCTCTGATTCAAACTGTCCAAG	55°C, 90 s
	hp2 VR	TGTTGCTGTGTTTTGCCTCT	
ΔHp3	hp3 KF	aggcaaaacacagcaacaaaagacacaccagaatcgcgcccgtatgcgttGTGTAGGCTGGAGCTGCTTC	68°C, 3 min
	hp3 KR	acagcgagaacaggagataagggatgaacggctgatacaggaacgcgaacCATATGAATATCCTCCTTAG	
	hp3 VF	GAATTGCCAGCCAGAGACAG	55°C, 90 s
	hp3 VR	GGTCATGCAGTTGAGTCAGC	
Δ*tonB*	tonB-KF	tgcatttaaaatcgagacctggtttttctactgaaatgattatgacttcaGTGTAGGCTGGAGCTGCTTC	68.6°C, 90 s
	tonB-KR	ctgttgagtaatagtcaaaagcctccggtcggaggcttttgactttctgcCATATGAATATCCTCCTTAG	
	tonB-VF	AACATACAACACGGGCACAA	54.9°C, 75 s
	tonB-VR	GACGACATCGGTCAGCATTA	
Δ*tolC*	tolC-KF	aattttacagtttgatcgcgctaaatactgcttcaccacaaggaatgcaaGTGTAGGCTGGAGCTGCTTC	64.5°C, 90 s
	tolC-KR	atctttacgttgccttacgttcagacggggccgaagccccgtcgtcgtcaCATATGAATATCCTCCTTAG	
	tolC-VF	CCAAATGTAACGGGCAGGTT	56°C, 2.5 min
	tolC-VR	GCGTGGCGTATGGATTTTGT	
pBAD18::*tolC*	pBAD18 tolC L insert	GCTAGCGAATTCGAGCTCGGTACCCGGGGGAATCCGCAATAATTTTACAGTTTGATCGCG	62°C, 2.5 min
	pBAD18 tolC R insert	GCTTGCATGCCTGCAGGTCGACTCTAGAGGATAACCCGTATCTTTACGTTGCCTTACG	
	pBAD18 tolC R plasmid	CGTAAGGCAACGTAAAGATACGGGTTATCCTCTAGAGTCGACCTGCAGGCATGCAAGC	62°C, 5 min
	pBAD18 tolC L plasmid	CGCGATCAAACTGTAAAATTATTGCGGATTCCCCCGGGTACCGAGCTCGAATTCGCTAGC	
	pBAD18 F	CTGTTTCTCCATACCCGTT	45°C, 2.25 min
	pBAD18 R	CTCATCCGCCAAAACAG	

(Continued on next page)

TABLE 2 (Continued)

Target(s)	Primer	Sequence	T_a, variable time
pBR322::p0.1229_3$^{2745–7950}$	pBR322 hp1 upstream L insert	GTATATATGAGTAAACTTGGTCTGACAGCATTAAAAGAGGCGTCAGAGGCAGAAAACG	56°C, 4 min
	pBR322 end 7 R insert	GCGGCATTTTGCCTTCCTGTTTTTGCGAAATCGGCAACGGTGATTCCCTATCAGGG	
	pBR322 end 7 R plasmid	CCCTGATAGGGAATCACCGTTGCCGATTTCGCAAAAACAGGAAGGCAAAATGCCGC	62°C, 4 min
	pBR322 hp1 upstream L plasmid	CGTTTTCTGCCTCTGACGCCTCTTTTAATGCTGTCAGACCAAGTTTACTCATATATAC	
	pBR322-F	TTTGCAAGCAGCAGATTACG	54.4°C, 2 min
	pBR322-R	GCCTCGTGATACGCCTATTT	

[a]T_a, amplification temperature; KF, knockout forward; KR, knockout reverse; VF, verification forward; VR, verification reverse. Note that for the KF or KR primers, the lowercase letters indicate regions homologous to the target gene, and the uppercase letters indicate the primer for the antibiotic resistance cassette. Superscript numbers indicate regions knocked out.

30 s, 49°C for 60 s, and 68°C for 100 s; 24 cycles of 95°C for 30 s, variable amplification temperatures (T_a) for 60 s, and 68°C at variable times; and a final extension step at 68°C for 5 min. T_a and variable times for each set of primers are reported in Table 2. The derivative pKD46-Kan^R was used instead of pKD46, as 0.1229 is resistant to ampicillin. Electroporation was used to construct *E. coli* 0.1229(pKD46) and MG1655(pKD46), using a Bio-Rad Gene Pulser II instrument according to protocols recommended by the manufacturer. Colonies containing pKD46-Kan^R were selected on LB plates with kanamycin. Strains containing pKD46 were grown to an OD_{600} of 0.3, and L-arabinose was added to a final concentration of 0.2 M. After incubation for 1 h, cells were washed and electroporated with the pKD3-derived PCR product. Transformants were selected on LB plates with chloramphenicol. Knockouts were confirmed by PCR using primers ~200 bp upstream and downstream of the gene, using standard PCR settings (initial denaturation step at 95°C for 30 s; 35 cycles of 95°C 30 s, variable T_a for 60 s, and 68°C at variable times; and a final extension step at 68°C for 5 min). This strategy was followed for all the knockouts, including primers and temperatures specific for each gene (Table 2).

Gibson cloning. The region spanning bp 2745 to 7950 of p0.1229_3 was cloned into pBR322 (pBR322::p0.1229_3$^{2745–7950}$), using Gibson cloning as previously described (70). Briefly, primer pairs containing 30 bp annealing to the pBR322 insert site and 30 bp that would anneal to p0.1229_3 were constructed. DNA from 0.1229 and pBR322 was amplified at these sites using standard PCR settings, and amplicons were cleaned up using a PCR purification kit (Qiagen, Germantown, MD) and subjected to assembly at 50°C using the Gibson cloning kit (New England Biosciences, Ipswich, MA). Assembled plasmids were propagated in DH5α competent cells (New England Biosciences, Ipswich, MA). Verification PCR was performed using primers 200 bp upstream and downstream of the insert site (Table 2) and confirmed using Sanger sequencing. Successful constructs were transformed into C600 electrocompetent cells. A similar process was used to clone *tolC* in pBAD18 (Kan^r).

Whole-genome sequencing and bioinformatics. For whole-genome sequencing of 0.1229, genomic DNA was isolated using the Wizard genomic DNA purification kit (Promega, Madison, WI). Whole-genome sequencing was performed at the Penn State Genomics Core facility using the Illumina MiSeq platform. A PCR-free DNA kit was used for library preparation. The sequencing run produced 2- by 150-bp reads.

For whole-genome sequencing of 99.0750, 91.0593, and 90.2723, genomic DNA was isolated using the Qiagen DNeasy blood and tissue kit (Qiagen Inc., Germantown, MD). Whole-genome sequencing was performed using the NexTera XT DNA library prep kit and run on an Illumina MiSeq platform. The sequencing run produced 2- by 250-bp reads.

After Illumina sequencing, Fastq files were checked using FastQC v0.11.5 (71) and assembled using SPAdes v3.10 (72). SPAdes assemblies were subjected to the Quality Assessment Tool for Genome Assemblies v4.5 (QUAST) (73), and contig number, genome size, N_{50}, and percent GC content (GC%) were noted.

Strain 0.1229 was also sequenced at the Center for Food Safety and Nutrition, Food and Drug Administration, using the PacBio RS II sequencing platform, as previously reported (74). For library preparation, 10 μg genomic DNA was sheared to 20-kb fragments by using g-tubes (Covaris Inc., Woburn, MA) according to the manufacturer's instructions. The SMRTbell 20-kb template library was constructed using DNA template prep kit 1.0 (Pacific Biosciences, Menlo Park, CA). BluePippin (Sage Science, Beverly, MA) was used for size selection, and sequencing was performed using P6/C4 chemistry on two single-molecule real-time (SMRT) cells, with a 240-min collection protocol along with stage start. SMRT Analysis 2.3.0 was used for read analysis, and *de novo* assembly was performed using the PacBio Hierarchical Genome Assembly Process (HGAP3.0) program. The assembly output from HGAP contained overlapping regions at the end, which can be identified using dot plots in Gepard (75). The genome was checked manually for even sequencing coverage. Afterwards, the improved consensus sequence was uploaded in SMRT Analysis 2.3.0 to determine the final consensus and accuracy scores using the Quiver consensus algorithm (76). The assembled genome was annotated using the NCBI's Prokaryotic Genomes Automatic Annotation Pipeline (PGAAP) (77).

Plasmid sequences were visualized using BLAST Ring Image Generator v0.95 (BRIG) (78). The Center for Genomic Epidemiology website was used for ResFinder v3.1.0 (90% identity and 60% length) (79), SerotypeFinder v2.0.1 (85% identity and 60% length) (80), and MLSTFinder v2.0.1 (81), using the multilocus sequence typing (MLST) scheme reported by Wirth et al. (82). The Integrated Microbial

Genomics and Microbiomes website of the DOE's Joint Genome Institute was utilized to perform BLAST analysis of the amino acid sequence of Hp1 against other genomes, and matches that were between 36 and 68% identical from various species were selected and then visualized using the gene neighborhood function (83).

Fastq files for 824 *E. coli* isolates were obtained using the BLAST+ (84) tool Fastq-dump. Strains were aligned to the nucleotide sequence of *hp1-abc-cupin* (bp 3094 to 6319 of p0.1229_3) using SRST2 (85). A cutoff of 90% nucleotide identity was used. Isolates 0.1229 and 91.0593 were used as positive controls.

Data analysis. MS Excel (Microsoft Corporation, Albuquerque, NM) was used to calculate the means, standard deviations, and standard errors, and Prism 6 (GraphPad Software, San Diego, CA) was used for generating figures. Error bars report standard errors of the means from at least three biological replicates.

Data availability. Nucleotide and SRA files for 0.1229 can be found in the NCBI database under BioSample accession number SAMN08737532. SRA files for 99.0750, 91.0593, and 90.2723 can be found under BioSample accession numbers SAMN11457477, SAMN11457478, and SAMN11457479, respectively.

SUPPLEMENTAL MATERIAL

Supplemental material is available online only.

SUPPLEMENTAL FILE 1, PDF file, 2.4 MB.

ACKNOWLEDGMENTS

We thank Craig Stephens at Santa Clara University for providing strain SF-173, Roberto Kolter at Harvard Medical School for providing strain ZK1526, and Erin Nawrocki for manuscript proofreading.

H.M.M. was supported by USDA National Needs grant 2014-38420-21822. This work was supported by grant 1 R21 AI130856-01A1 through the National Institute of Allergy and Infectious Diseases and USDA National Institute of Food and Agriculture Federal Appropriations under project PEN04522s and accession number 0233376.

REFERENCES

1. Griffin PM, Tauxe RV. 1991. The epidemiology of infections caused by *Escherichia coli* O157:H7, other enterohemorrhagic *E. coli*, and the associated hemolytic uremic syndrome. Epidemiol Rev 13:60–98. https://doi.org/10.1093/oxfordjournals.epirev.a036079.
2. Nguyen Y, Sperandio V, Padola NL, Starai VJ. 2012. Enterohemorrhagic *E. coli* (EHEC) pathogenesis. Front Cell Infect Microbiol 2:90. https://doi.org/10.3389/fcimb.2012.00090.
3. Hayashi T, Makino K, Ohnishi M, Kurokawa K, Ishii K, Yokoyama K, Han C-G, Ohtsubo E, Nakayama K, Murata T, Tanaka M, Tobe T, Iida T, Takami H, Honda T, Sasakawa C, Ogasawara N, Yasunaga T, Kuhara S, Shiba T, Hattori M, Shinagawa H. 2001. Complete genome sequence of enterohemorrhagic *Escherichia coli* O157:H7 and genomic comparison with a laboratory strain K-12. DNA Res 8:11–22. https://doi.org/10.1093/dnares/8.1.11.
4. Waldor MK, Friedman DI. 2005. Phage regulatory circuits and virulence gene expression. Curr Opin Microbiol 8:459–465. https://doi.org/10.1016/j.mib.2005.06.001.
5. Zhang X, McDaniel AD, Wolf LE, Keusch GT, Waldor MK, Acheson DW. 2000. Quinolone antibiotics induce Shiga toxin-encoding bacteriophages, toxin production, and death in mice. J Infect Dis 181:664–670. https://doi.org/10.1086/315239.
6. Scotland S, Smith HR, Rowe B. 1985. Two distinct toxins active on Vero cells from *Escherichia coli* O157. Lancet ii:885–886. https://doi.org/10.1016/s0140-6736(85)90146-1.
7. Scheutz F, Teel LD, Beutin L, Piérard D, Buvens G, Karch H, Mellmann A, Caprioli A, Tozzoli R, Morabito S, Strockbine NA, Melton-Celsa AR, Sanchez M, Persson S, O'Brien AD. 2012. Multicenter evaluation of a sequence-based protocol for subtyping Shiga toxins and standardizing Stx nomenclature. J Clin Microbiol 50:2951–2963. https://doi.org/10.1128/JCM.00860-12.
8. Bai X, Fu S, Zhang J, Fan R, Xu Y, Sun H, He X, Xu J, Xiong Y. 2018. Identification and pathogenomic analysis of an *Escherichia coli* strain producing a novel Shiga toxin 2 subtype. Sci Rep 8:6756. https://doi.org/10.1038/s41598-018-25233-x.
9. FAO/WHO STEC Expert Group. 2019. Hazard identification and characterization: criteria for categorizing Shiga toxin-producing *Escherichia coli* on a risk basis. J Food Prot 82:7–21. https://doi.org/10.4315/0362-028X.JFP-18-291.
10. Strockbine NA, Marques LR, Newland JW, Smith HW, Holmes RK, O'Brien AD. 1986. Two toxin-converting phages from *Escherichia coli* O157:H7 strain 933 encode antigenically distinct toxins with similar biologic activities. Infect Immun 53:135–140.
11. Matsushiro A, Sato K, Miyamoto H, Yamamura T, Honda T. 1999. Induction of prophages of enterohemorrhagic *Escherichia coli* O157:H7 with norfloxacin. J Bacteriol 181:2257–2260.
12. Ostroff S, Tarr P, Neill MA, Lewis JH, Hargrett-Bean N, Kobayashi JM. 1989. Toxin genotypes and plasmid profiles as determinants of systemic sequelae in *Escherichia coli* O157:H7 infections. J Infect Dis 160:994–998. https://doi.org/10.1093/infdis/160.6.994.
13. Donohue-Rolfe A, Kondova I, Oswald S, Hutto D, Tzipori S. 2000. *Escherichia coli* O157:H7 strains that express Shiga toxin (Stx) 2 alone are more neurotropic for gnotobiotic piglets than are isotypes producing only Stx1 or both Stx1 and Stx2. J Infect Dis 181:1825–1829. https://doi.org/10.1086/315421.
14. Orth D, Grif K, Khan AB, Naim A, Dierich MP, Würzner R. 2007. The Shiga toxin genotype rather than the amount of Shiga toxin or the cytotoxicity of Shiga toxin *in vitro* correlates with the appearance of the hemolytic uremic syndrome. Diagn Microbiol Infect Dis 59:235–242. https://doi.org/10.1016/j.diagmicrobio.2007.04.013.
15. Persson S, Olsen KEP, Ethelberg S, Scheutz F. 2007. Subtyping method for *Escherichia coli* Shiga toxin (verocytotoxin) 2 variants and correlations to clinical manifestations. J Clin Microbiol 45:2020–2024. https://doi.org/10.1128/JCM.02591-06.
16. Shringi S, Schmidt C, Katherine K, Brayton KA, Hancock DD, Besser TE. 2012. Carriage of *stx2a* differentiates clinical and bovine-biased strains of *Escherichia coli* O157. PLoS One 7:e51572. https://doi.org/10.1371/journal.pone.0051572.
17. Kawano K, Okada M, Haga T, Maeda K, Goto Y. 2008. Relationship between pathogenicity for humans and *stx* genotype in Shiga toxin-producing *Escherichia coli* serotype O157. Eur J Clin Microbiol Infect Dis 27:227–232. https://doi.org/10.1007/s10096-007-0420-3.
18. FAO/WHO. 2018. Shiga toxin-producing Escherichia coli (STEC) and food: attribution, characterization, and monitoring. FAO/WHO, Rome, Italy.
19. Carey CM, Kostrzynska M, Ojha S, Thompson S. 2008. The effect of probiotics and organic acids on Shiga-toxin 2 gene expression in enterohemorrhagic *Escherichia coli* O157:H7. J Microbiol Methods 73:125–132. https://doi.org/10.1016/j.mimet.2008.01.014.
20. Thévenot J, Cordonnier C, Rougeron A, Le Goff O, Nguyen HTT, Denis S,

Alric M, Livrelli V, Blanquet-Diot S. 2015. Enterohemorrhagic *Escherichia coli* infection has donor-dependent effect on human gut microbiota and may be antagonized by probiotic yeast during interaction with Peyer's patches. Appl Microbiol Biotechnol 99:9097–9110. https://doi.org/10.1007/s00253-015-6704-0.
21. de Sablet T, Chassard C, Bernalier-Donadille A, Vareille M, Gobert AP, Martin C. 2009. Human microbiota-secreted factors inhibit Shiga toxin synthesis by enterohemorrhagic *Escherichia coli* O157:H7. Infect Immun 77:783–790. https://doi.org/10.1128/IAI.01048-08.
22. Gamage SD, Strasser JE, Chalk CL, Weiss AA. 2003. Nonpathogenic *Escherichia coli* can contribute to the production of Shiga toxin. Infect Immun 71:3107–3115. https://doi.org/10.1128/iai.71.6.3107-3115.2003.
23. Goswami K, Chen C, Xiaoli L, Eaton KA, Dudley EG. 2015. Coculture of *Escherichia coli* O157:H7 with a nonpathogenic *E. coli* strain increases toxin production and virulence in a germfree mouse model. Infect Immun 83:4185–4193. https://doi.org/10.1128/IAI.00663-15.
24. Xiaoli L, Figler HM, Goswami K, Dudley EG. 2018. Nonpathogenic *E. coli* enhance Stx2a production of *E. coli* O157:H7 through *bamA*-dependent and independent mechanisms. Front Microbiol 9:1325. https://doi.org/10.3389/fmicb.2018.01325.
25. Smith DL, James CE, Sergeant MJ, Yaxian Y, Saunders JR, McCarthy AJ, Allison HE. 2007. Short-tailed Stx phages exploit the conserved YaeT protein to disseminate Shiga toxin genes among enterobacteria. J Bacteriol 189:7223–7233. https://doi.org/10.1128/JB.00824-07.
26. Rasko DA, Moreira CG, Li DR, Reading NC, Ritchie JM, Waldor MK, Williams N, Taussig R, Wei S, Roth M, Hughes DT, Huntley JF, Fina MW, Falck JR, Sperandio V. 2008. Targeting QseC signaling and virulence for antibiotic development. Science 321:1078–1080. https://doi.org/10.1126/science.1160354.
27. Toshima H, Yoshimura A, Arikawa K, Hidaka A, Ogasawara J, Hase A, Masaki H, Nishikawa Y. 2007. Enhancement of Shiga toxin production in enterohemorrhagic *Escherichia coli* serotype O157:H7 by DNase colicins. Appl Environ Microbiol 73:7582–7588. https://doi.org/10.1128/AEM.01326-07.
28. Mobley HLT, Green DM, Trifillis AL, Johnson DE, Chippendale GR, Lockatell CV, Jones BD, Warren JW. 1990. Pyelonephritogenic *Escherichia coli* and killing of cultured human renal proximal tubular epithelial cells: role of hemolysin in some strains. Infect Immun 58:1281–1289.
29. Nissle A. 1919. More about the Mutaflor treatment with special consideration of the chronic dysentery. Munch Med Wochenschr 25:678–681.
30. Wijetunge DSS, Karunathilake KHEM, Chaudhari A, Katani R, Dudley EG, Kapur V, DebRoy C, Kariyawasam S. 2014. Complete nucleotide sequence of pRS218, a large virulence plasmid, that augments pathogenic potential of meningitis-associated *Escherichia coli* strain RS218. BMC Microbiol 14:203. https://doi.org/10.1186/s12866-014-0203-9.
31. Chen SL, Hung C-S, Xu J, Reigstad CS, Magrini V, Sabo A, Blasiar D, Bieri T, Meye RR, Ozersky P, Armstrong JR, Fulton RS, Latreille JP, Spieth J, Hooton TM, Mardis ER, Hultgren SJ, Gordon JI. 2006. Identification of genes subject to positive selection in uropathogenic strains of *Escherichia coli*: a comparative genomics approach. Proc Natl Acad Sci U S A 103:5977–5982. https://doi.org/10.1073/pnas.0600938103.
32. Davagnino J, Herrero M, Furlong D, Moreno F, Kolter R. 1986. The DNA replication inhibitor microcin B17 is a forty-three-amino-acid protein containing sixty percent glycine. Proteins Struct Funct Genet 1:230–238. https://doi.org/10.1002/prot.340010305.
33. Stephens CM, Skerker CM, Sekhon JM, Arkin MS, Riley AP. 2015. Complete genome sequences of four *Escherichia coli* ST95 isolates from bloodstream infections. Genome Announc 3:e01241-15. https://doi.org/10.1128/genomeA.01241-15.
34. Künne C, Billion A, Mshana SE, Schmiedel J, Domann E, Hossain H, Hain T, Imirzalioglu C, Chakraborty T. 2012. Complete sequences of plasmids from the hemolytic-uremic syndrome-associated *Escherichia coli* strain HUSEC41. J Bacteriol 194:532–533. https://doi.org/10.1128/JB.06368-11.
35. Thompson RE, Collin F, Maxwell A, Jolliffe KA, Payne RJ. 2014. Synthesis of full length and truncated microcin B17 analogues as DNA gyrase poisons. Org Biomol Chem 12:1570–1578. https://doi.org/10.1039/c3ob42516a.
36. Delgado MA, Solbiati JO, Chiuchiolo MJ, Farías RN, Salomón RA. 1999. *Escherichia coli* outer membrane protein TolC is involved in production of the peptide antibiotic microcin J25. J Bacteriol 181:1968–1970.
37. Braun V, Patzer SI, Hantke K. 2002. Ton-dependent colicins and microcins: modular design and evolution. Biochimie 84:365–380. https://doi.org/10.1016/s0300-9084(02)01427-x.
38. Penders J, Thijs C, Vink C, Stelma FF, Snijders B, Kummeling I, van den Brandt PA, Stobberingh EE. 2006. Factors influencing the composition of the intestinal microbiota in early infancy. Pediatrics 118:511–521. https://doi.org/10.1542/peds.2005-2824.
39. Slanetz LW, Bartley CH. 1957. Numbers of enterococci in water, sewage, and feces determined by the membrane filter technique with an improved medium. J Bacteriol 74:591–595.
40. Apperloo-Renkema HZ, Van Der Waaij BD, Van Der Waaij D. 1990. Determination of colonization resistance of the digestive tract by biotyping of Enterobacteriaceae. Epidemiol Infect 105:355–361. https://doi.org/10.1017/s0950268800047944.
41. Johnson JR, Owens K, Gajewski A, Clabots C. 2008. *Escherichia coli* colonization patterns among human household members and pets, with attention to acute urinary tract infection. J Infect Dis 197:218–224. https://doi.org/10.1086/524844.
42. Leatham MP, Banerjee S, Autieri SM, Conway T, Cohen PS, Mercado-Lubo R. 2009. Precolonized human commensal *Escherichia coli* strains serve as a barrier to *E. coli* O157:H7 growth in the streptomycin-treated mouse intestine. Infect Immun 77:2876–2886. https://doi.org/10.1128/IAI.00059-09.
43. Sperandio V, Mellies JL, Nguyen W, Shin S, Kaper JB. 1999. Quorum sensing controls expression of the type III secretion gene transcription and protein secretion in enterohemorrhagic and enteropathogenic *Escherichia coli*. Proc Natl Acad Sci U S A 96:15196–15201. https://doi.org/10.1073/pnas.96.26.15196.
44. Sperandio V, Torres AG, Gir NJA, Kaper JB. 2001. Quorum sensing is a global regulatory mechanism in enterohemorrhagic *Escherichia coli* O157:H7. J Bacteriol 183:5187–5197. https://doi.org/10.1128/jb.183.17.5187-5197.2001.
45. Zhao T, Doyle MP, Harmon BG, Brown CA, Mueller PO, Parks AH. 1998. Reduction of carriage of enterohemorrhagic *Escherichia coli* O157:H7 in cattle by inoculation with probiotic bacteria. J Clin Microbiol 36:641–647.
46. Bell BP, Griffin PM, Lozano P, Christie DL, Kobayashi JM, Tarr PI. 1997. Predictors of hemolytic uremic syndrome in children during a large outbreak of *Escherichia coli* O157:H7 infections. Pediatrics 100:E12. https://doi.org/10.1542/peds.100.1.e12.
47. Gamage SD, Patton AK, Strasser JE, Chalk CL, Weiss AA. 2006. Commensal bacteria influence *Escherichia coli* O157:H7 persistence and Shiga toxin production in the mouse intestine. Infect Immun 74:1977–1983. https://doi.org/10.1128/IAI.74.3.1977-1983.2006.
48. Amigo N, Mercado E, Bentancor A, Singh P, Vilte D, Gerhardt E, Zotta E, Ibarra C, Manning SD, Larzábal M, Cataldi A. 2015. Clade 8 and clade 6 strains of *Escherichia coli* O157:H7 from cattle in Argentina have hypervirulent-like phenotypes. PLoS One 10:e0127710. https://doi.org/10.1371/journal.pone.0127710.
49. Micenková L. 2016. Bacteriocinogeny in pathogenic and commensal *Escherichia coli* strains. Masarykova Univerzita Lékařská Fakulta Biologický Ústav, Brno, Czechia.
50. Bielaszewska M, Idelevich EA, Zhang W, Bauwens A, Schaumburg F, Mellmann A, Peters G, Karch H. 2012. Effects of antibiotics on Shiga toxin 2 production and bacteriophage induction by epidemic *Escherichia coli* O104:H4 strain. Antimicrob Agents Chemother 56:3277–3282. https://doi.org/10.1128/AAC.06315-11.
51. Łoś JM, Łoś M, Węgrzyn A, Węgrzyn G. 2010. Hydrogen peroxide-mediated induction of the Shiga toxin converting lambdoid prophage ST2-8624 in *Escherichia coli* O157:H7. FEMS Immunol Med Microbiol 58:322–329. https://doi.org/10.1111/j.1574-695X.2009.00644.x.
52. Cascales E, Buchanan SK, Duche D, Kleanthous C, Lloubes R, Postle K, Riley M, Slatin S, Cavard D. 2007. Colicin biology. Microbiol Mol Biol Rev 71:158–229. https://doi.org/10.1128/MMBR.00036-06.
53. Duquesne S, Destoumieux-Garzón D, Peduzzi J, Rebuffat S. 2007. Microcins, gene-encoded antibacterial peptides from enterobacteria. Nat Prod Rep 24:708–734. https://doi.org/10.1039/b516237h.
54. Patzer SI, Baquero MR, Bravo D, Moreno F, Hantke K. 2003. The colicin G, H and X determinants encode microcins M and H47, which might utilize the catecholate siderophore receptors FepA, Cir, Fiu and IroN. Microbiology 149:2557–2570. https://doi.org/10.1099/mic.0.26396-0.
55. Gilson L, Mahanty K, Kolter R. 1987. Four plasmid genes are required for colicin V synthesis, export, and immunity. J Bacteriol 169:2466–2470. https://doi.org/10.1128/jb.169.6.2466-2470.1987.
56. Chehade H, Braun V. 1988. Iron-regulated synthesis and uptake of colicin V. FEMS Microbiol Lett 52:177–181. https://doi.org/10.1111/j.1574-6968.1988.tb02591.x.
57. Corsini G, Karahanian E, Tello M, Fernandez K, Rivero D, Saavedra JM, Ferrer A. 2010. Purification and characterization of the antimicrobial

peptide microcin N. FEMS Microbiol Lett 312:119–125. https://doi.org/10.1111/j.1574-6968.2010.02106.x.
58. Morin N, Lanneluc I, Connil N, Cottenceau M, Pons AM, Sablé S. 2011. Mechanism of bactericidal activity of microcin L in *Escherichia coli* and *Salmonella enterica*. Antimicrob Agents Chemother 55:997–1007. https://doi.org/10.1128/AAC.01217-10.
59. Eberhart LJ, Deringer JR, Brayton KA, Sawant AA, Besser TE, Call DR. 2012. Characterization of a novel microcin that kills enterohemorrhagic *Escherichia coli* O157:H7 and O26. Appl Environ Microbiol 78:6592–6599. https://doi.org/10.1128/AEM.01067-12.
60. Zhao Z, Orfe LH, Liu J, Lu S-Y, Besser TE, Call DR. 2017. Microcin PDI regulation and proteolytic cleavage are unique among known microcins. Sci Rep 7:42529. https://doi.org/10.1038/srep42529.
61. Havarstein LS, Holo H, Nes IF. 1994. The leader peptide of colicin V shares consensus sequences with leader peptides that are common among peptide bacteriocins produced by Gram-positive bacteria. Microbiology 140:2383–2389. https://doi.org/10.1099/13500872-140-9-2383.
62. Havarstein LS, Diep DB, Nes IF. 1995. A family of bacteriocin ABC transporters carry out proteolytic processing of their substrates concomitant with export. Mol Microbiol 16:229–240. https://doi.org/10.1111/j.1365-2958.1995.tb02295.x.
63. Yang CC, Konisky J. 1984. Colicin V-treated *Escherichia coli* does not generate membrane potential. J Bacteriol 158:757–759.
64. Yuzenkova J, Delgado M, Nechaev S, Savalia D, Epshtein V, Artsimovitch I, Mooney RA, Landick R, Farias RN, Salomon R, Severinov K. 2002. Mutations of bacterial RNA polymerase leading to resistance to microcin J25. J Biol Chem 277:50867–50875. https://doi.org/10.1074/jbc.M209425200.
65. Gilson L, Mahanty HK, Kolter R. 1990. Genetic analysis of an MDR-like export system: the secretion of colicin V. EMBO J 9:3875–3884. https://doi.org/10.1002/j.1460-2075.1990.tb07606.x.
66. Hartzell A, Chen C, Lewis C, Liu K, Reynolds S, Dudley EG. 2011. *Escherichia coli* O157:H7 of genotype lineage-specific polymorphism assay 211111 and clade 8 are common clinical isolates within Pennsylvania. Foodborne Pathog Dis 8:763–768. https://doi.org/10.1089/fpd.2010.0762.
67. Zaslaver A, Bren A, Ronen M, Itzkovitz S, Kikoin I, Shavit S, Liebermeister W, Surette MG, Alon U. 2006. A comprehensive library of fluorescent transcriptional reporters for *Escherichia coli*. Nat Methods 3:623–628. https://doi.org/10.1038/nmeth895.
68. Fan J, de Jonge BLM, MacCormack K, Sriram S, McLaughlin RE, Plant H, Preston M, Fleming PR, Albert R, Foulk M, Mills SD. 2014. A novel high-throughput cell-based assay aimed at identifying inhibitors of DNA metabolism in bacteria. Antimicrob Agents Chemother 58:7264–7272. https://doi.org/10.1128/AAC.03475-14.
69. Datsenko K, Wanner BL. 2000. One-step inactivation of chromosomal genes in *Escherichia coli* K-12 using PCR products. Proc Natl Acad Sci U S A 97:6640–6645. https://doi.org/10.1073/pnas.120163297.
70. Gibson DG, Young L, Chuang R-Y, Venter JC, Hutchison CA, Smith HO. 2009. Enzymatic assembly of DNA molecules up to several hundred kilobases. Nat Methods 6:343–345. https://doi.org/10.1038/nmeth.1318.
71. Andrews S. 2010. FastQC: a quality control tool for high throughput sequence data. Babraham Institute, Cambridge, United Kingdom.
72. Bankevich A, Nurk S, Antipov D, Gurevich AA, Dvorkin M, Kulikov AS, Lesin VM, Nikolenko SI, Pham S, Prjibelski AD, Pyshkin AV, Sirotkin AV, Vyahhi N, Tesler G, Alekseyev MA, Pevzner PA. 2012. SPAdes: a new genome assembly algorithm and its applications to single-cell sequencing. J Comput Biol 19:455–477. https://doi.org/10.1089/cmb.2012.0021.
73. Gurevich A, Saveliev V, Vyahhi N, Tesler G. 2013. QUAST: quality assessment tool for genome assemblies. Bioinformatics 29:1072–1075. https://doi.org/10.1093/bioinformatics/btt086.
74. Yao K, Roberts RJ, Allard MW, Hoffmann M. 2017. Complete genome and methylome sequences of *Salmonella enterica* subsp. *enterica* serovars Typhimurium, Saintpaul, and Stanleyville from the SARA/SARB collection. Genome Announc 5:e00031-17. https://doi.org/10.1128/genomeA.00031-17.
75. Krumsiek J, Arnold R, Rattei T. 2007. Gepard: a rapid and sensitive tool for creating dotplots on genome scale. Bioinformatics 23:1026–1028. https://doi.org/10.1093/bioinformatics/btm039.
76. Chin C-S, Alexander DH, Marks P, Klammer AA, Drake J, Heiner C, Clum A, Copeland A, Huddleston J, Eichler EE, Turner SW, Korlach J. 2013. Nonhybrid, finished microbial genome assemblies from long-read SMRT sequencing data. Nat Methods 10:563–569. https://doi.org/10.1038/nmeth.2474.
77. Klimke W, Agarwala R, Badretdin A, Chetvernin S, Ciufo S, Fedorov B, Kiryutin B, O'Neill K, Resch W, Resenchuk S, Schafer S, Tolstoy I, Tatusova T. 2009. The National Center for Biotechnology Information's Protein Clusters Database. Nucleic Acids Res 37:D216–D223. https://doi.org/10.1093/nar/gkn734.
78. Alikhan N-F, Petty NK, Ben Zakour NL, Beatson SA. 2011. BLAST Ring Image Generator (BRIG): simple prokaryote genome comparisons. BMC Genomics 12:402. https://doi.org/10.1186/1471-2164-12-402.
79. Zankari E, Hasman H, Cosentino S, Vestergaard M, Rasmussen S, Lund O, Aarestrup FM, Larsen MV. 2012. Identification of acquired antimicrobial resistance genes. J Antimicrob Chemother 67:2640–2644. https://doi.org/10.1093/jac/dks261.
80. Joensen KG, Tetzschner AMM, Iguchi A, Aarestrup FM, Scheutz F. 2015. Rapid and easy in silico serotyping of *Escherichia coli* isolates by use of whole-genome sequencing data. J Clin Microbiol 53:2410–2426. https://doi.org/10.1128/JCM.00008-15.
81. Larsen MV, Cosentino S, Rasmussen S, Friis C, Hasman H, Marvig RL, Jelsbak L, Sicheritz-Pontén T, Ussery DW, Aarestrup FM, Lund O. 2012. Multilocus sequence typing of total-genome-sequenced bacteria. J Clin Microbiol 50:1355–1361. https://doi.org/10.1128/JCM.06094-11.
82. Wirth T, Falush D, Lan R, Colles F, Mensa P, Wieler LH, Karch H, Reeves PR, Maiden MCJ, Ochman H, Achtman M. 2006. Sex and virulence in *Escherichia coli*: an evolutionary perspective. Mol Microbiol 60:1136–1151. https://doi.org/10.1111/j.1365-2958.2006.05172.x.
83. Chen I-MA, Chu K, Palaniappan K, Pillay M, Ratner A, Huang J, Huntemann M, Varghese N, White JR, Seshadri R, Smirnova T, Kirton E, Jungbluth SP, Woyke T, Eloe-Fadrosh EA, Ivanova NN, Kyrpides NC. 2019. IMG/M v.5.0: an integrated data management and comparative analysis system for microbial genomes and microbiomes. Nucleic Acids Res 47:D666–D677. https://doi.org/10.1093/nar/gky901.
84. Camacho C, Coulouris G, Avagyan V, Ma N, Papadopoulos J, Bealer K, Madden TL. 2009. BLAST+: architecture and applications. BMC Bioinformatics 10:421. https://doi.org/10.1186/1471-2105-10-421.
85. Inouye M, Dashnow H, Raven L-A, Schultz MB, Pope BJ, Tomita T, Zobel J, Holt KE. 2014. SRST2: rapid genomic surveillance for public health and hospital microbiology labs. Genome Med 6:90. https://doi.org/10.1186/s13073-014-0090-6.
86. Riley LW, Remis RS, Helgerson SD, McGee HB, Wells JG, Davis BR, Hebert RJ, Olcott ES, Johnson LM, Hargrett NT, Blake PA, Cohen ML. 1983. Hemorrhagic colitis associated with a rare *Escherichia coli* serotype. N Engl J Med 308:681–685. https://doi.org/10.1056/NEJM198303243081203.
87. Appleyard RK. 1954. Segregation of new lysogenic types during growth of a doubly lysogenic strain derived from Escherichia coli K12. Genetics 39:440–452.
88. Blattner FR, Plunkett G, Bloch CA, Perna NT, Burland V, Riley M, Collado-Vides J, Glasner JD, Rode CK, Mayhew GF, Gregor J, Davis NW, Kirkpatrick HA, Goeden MA, Rose DJ, Mau B, Shao Y. 1997. The complete genome sequence of *Escherichia coli* K-12. Science 277:1453–1462. https://doi.org/10.1126/science.277.5331.1453.
89. Achtman M, Mercer A, Kusecek B, Pohl A, Heuzenroeder M, Aaronson W, Sutton A, Silver RP. 1983. Six widespread bacterial clones among *Escherichia coli* K1 isolates. Infect Immun 39:315–335.
90. Yorgey P, Lee J, Kördel J, Vivas E, Warner P, Jebaratnam D, Kolter R. 1994. Posttranslational modifications in microcin B17 define an additional class of DNA gyrase inhibitor. Proc Natl Acad Sci U S A 91:4519–4523. https://doi.org/10.1073/pnas.91.10.4519.
91. Guzman L-M, Belin D, Carson MJ, Beckwith J. 1995. Tight regulation, modulation, and high-level expression by vectors containing the arabinose pBAD promoter. J Bacteriol 177:4121–4130. https://doi.org/10.1128/jb.177.14.4121-4130.1995.
92. Larsen RA, Thomas MG, Postle K. 1999. Protonmotive force, ExbB and ligand-bound FepA drive conformational changes in TonB. Mol Microbiol 31:1809–1824. https://doi.org/10.1046/j.1365-2958.1999.01317.x.
93. Bolivar F, Rodriguez RL, Greene PJ, Betlach MC, Heyneker HL, Boyer HW, Crosa JH, Falkow S. 1977. Construction and characterization of new cloning vehicle. II. A multipurpose cloning system. Gene 2:95–113. https://doi.org/10.1016/0378-1119(77)90000-2.
94. Rebuffat S. 2012. Microcins in action: amazing defence strategies of enterobacteria. Biochem Soc Trans 40:1456–1462. https://doi.org/10.1042/BST20120183.